A Thermal Spin Transition in $[Co(bpy)_3][LiCr(ox)_3]$ ($ox = C_2O_4^{2-}$; bpy = 2,2′-bipyridine)

Regula Sieber,[b] Silvio Decurtins,[b] Helen Stoeckli-Evans,[c] Claire Wilson,[d] Dima Yufit,[d] Judith A. K. Howard,[d] Silvia C. Capelli,[e] and Andreas Hauser[a]*

Dedicated to Professor Philipp Gütlich on the occasion of his 65th birthday

Abstract: In the three-dimensional oxalate network structures $[M^{II}(bpy)_3][M^{I}M^{III}(ox)_3]$ ($ox = C_2O_4^{2-}$; bpy = 2,2′-bipyridine) the negatively charged oxalate backbone provides perfect cavities for tris-bipyridyl complex cations. The size of the cavity can be adjusted by variation of the metal ions of the oxalate backbone. In $[Co(bpy)_3][NaCr(ox)_3]$, the $[Co(bpy)_3]2+$ complex is in its usual $^4T_1(t_{2g}^5e_g^2)$ high-spin ground state. Substituting Na^+ by Li^+ reduces the size of the cavity. The resulting chemical pressure destabilises the high-spin state of $[Co(bpy)_3]^{2+}$ to such an extent that the $^2E(t_{2g}^6e_g^1)$ low-spin state becomes the actual ground state. As a result, $[Co(bpy)_3][LiCr(ox)_3]$ becomes a spin-crossover system, as shown by temperature-dependent magnetic susceptibility measurements and single-crystal optical spectroscopy, as well as by an X-ray structure determination at 290 and 10 K.

Keywords: cobalt · magnetic properties · N ligands · optical properties · oxalate networks · spin crossover

Introduction

The three-dimensional oxalate networks of the type $[M^{II}(bpy)_3][M^{I}M^{III}(ox)_3]$ possess a very intriguing crystal structure.[1] The $[M^{III}(ox)_3]^{3-}$ complexes are held together by the M^I cations to form a three-dimensional, negatively charged backbone of cubic symmetry, with each oxalate ion acting as a bridging ligand. The rather loose network is actively stabilised by the $[M^{II}(bpy)_3]^{2+}$ counter ions that sit in the cavities provided by the network. This results in an extremely tightly packed crystal structure. The M^I cations are preferably Li^+ and Na^+. It is, however, possible to combine a large number of different divalent and trivalent metal ions on the M^{II} and M^{III} sites, respectively, as long as elementary rules regarding relative stability constants and redox potentials of the components are obeyed and some geometric restrictions are taken into account. The various combinations lead to interesting magnetic[2] and photophysical[3] phenomena.

Recently, Tiwary and Vasudevan[4] took up the idea of Mizuno and Lunsford,[5] and reported that $[Co(bpy)_3]^{2+}$, which normally has a $^4T_1(t_{2g}^5e_g^2)$ high-spin ground state,[6] becomes a spin-crossover complex when incorporated into the cavities of zeolite-Y. They attributed the necessary destabilisation of the high-spin state relative to the $^2E(t_{2g}^6e_g^1)$ low-spin state to a geometric distortion imposed on the $[Co(bpy)_3]^{2+}$ complexes by the charge distribution inside the zeolite cavity.

In the three-dimensional oxalate networks, the size of the cavity of the $[M^{II}(bpy)_3]^{2+}$ site can be adjusted by variation of the metal ions on the oxalate backbone. In this paper we explore the possibility of inducing a thermal spin transition in $[Co(bpy)_3]^{2+}$, incorporated as a complex cation in the oxalate network, by such variation. We present and discuss the results of magnetic susceptibility measurements, single-crystal optical spectroscopy, and X-ray crystal structure determinations on $[Co(bpy)_3][NaCr(ox)_3]$ and $[Co(bpy)_3][LiCr(ox)_3]$, as well as for comparison on $[Zn(bpy)_3][NaCr(ox)_3]$ and $[Ru(bpy)_3][LiCr(ox)_3]$.

[a] Prof. Dr. A. Hauser
Département de chimie physique
Université de Genève, 30 Quai Ernest-Ansermet
CH-1211 Genève 4 (Switzerland)
Fax: (+41) 22-702-6103
E-mail: andreas.hauser@chiphy.unige.ch

[b] R. Sieber, Prof. Dr. S. Decurtins
Departement für Chemie und Biochemie
Universität Bern, Freiestrasse 3
CH-3000 Bern 9 (Switzerland)

[c] Prof. Dr. H. Stoeckli-Evans
Institut de chimie
Université de Neuchâtel, 51 Avenue de Bellevaux
CH-2000 Neuchâtel (Switzerland)

[d] C. Wilson, D. Yufit, Prof. Dr. J. A. K. Howard
Department of Chemistry
University of Durham
Durham DH1 3LE (UK)

[e] Dr. S. C. Capelli
Institut für chemische Kristallographie
Universität Bern, Freiestrasse 3
CH-3000 Bern 9 (Switzerland)

  0947-6539/00/0602-0361 $ 17.50+.50/0

Results

Structure determination: The three-dimensional network structures of the type $[M^{II}(bpy)_3][M^{I}M^{III}(ox)_3]$ crystallise in the cubic space group $P2_13$, $Z = 4$.[1] The relevant single crystal data and parameters regarding the data collection and structure refinements for the compounds $[Co(bpy)_3][NaCr(ox)_3]$, $[Co(bpy)_3][LiCr(ox)_3]$ and $[Zn(bpy)_3][NaCr(ox)_3]$ at room temperature as well as for $[Co(bpy)_3][LiCr(ox)_3]$ at 10 K and $[Ru(bpy)_3][LiCr(ox)_3]$ at 100 K are given in Table 1. Whereas for $[Ru(bpy)_3][LiCr(ox)_3]$ there is spectroscopic evidence for a slight lowering of the symmetry at low temperatures,[7] $[Co(bpy)_3][LiCr(ox)_3]$ stays in the $P2_13$ space group down to 10 K. The general features of the crystal structure have been reported previously. As depicted in Figure 1, it consists of the three-dimensional oxalate backbone, which provides perfect cavities with regard to size and geometry for the $[M^{II}(bpy)_3]^{2+}$ ions. The site symmetry of both the tris-oxalate as well as the tris-bipyridyl complexes is C_3. The rather loose oxalate network is actively stabilised by the tris-bipyridyl complexes through electrostatic interactions from π-overlap between oxalate and bipyridine along the trigonal axis.

In Table 2, selected metal–ligand bond lengths and angles are given for $[Zn(bpy)_3][NaCr(ox)_3]$, $[Co(bpy)_3][NaCr(ox)_3]$ and $[Co(bpy)_3][LiCr(ox)_3]$ at room temperature, as well as for $[Co(bpy)_3][LiCr(ox)_3]$ at 10 K and $[Ru(bpy)_3][LiCr(ox)_3]$ at 100 K. Naturally, there is a large difference in M^{I}–O bond lengths between the compounds containing Na^+ and Li^+, but they are quite similar for the two Na^+ compounds and the two Li^+ compounds, respectively. The Cr–O bond lengths, on the other hand, span the comparatively small range of 1.963 to 1.981 Å for the four compounds, and for $[Co(bpy)_3][LiCr(ox)_3]$ the temperature dependence is negligible. The M^{II}–N

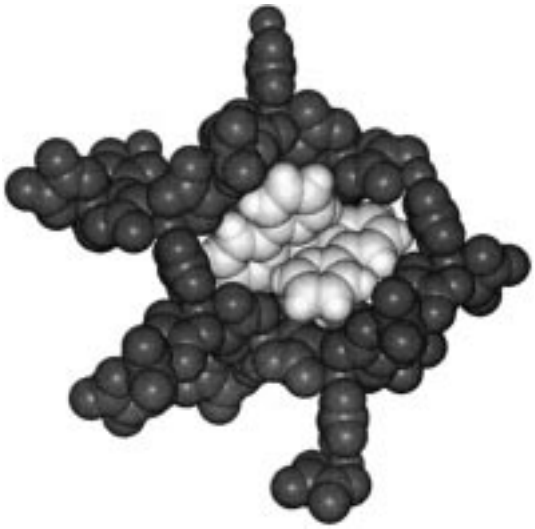

Figure 1. View of one $[M^{II}(bpy)_3]^{2+}$ complex that sits in the cavity provided by the $[M^{I}M^{III}(ox)_3]^{2-}$ network.

Table 1. Crystallographic data and structure refinement for the three compounds $[Zn(bpy)_3][NaCr(ox)_3]$, $[Co(bpy)_3][NaCr(ox)_3]$ and $[Co(bpy)_3][LiCr(ox)_3]$ at 293 K as well as for $[Co(bpy)_3][LiCr(ox)_3]$ at 10 K and $[Ru(bpy)_3][LiCr(ox)_3]$ at 100 K.

	$[Zn(bpy)_3][NaCr(ox)_3]$	$[Co(bpy)_3][NaCr(ox)_3]$	$[Co(bpy)_3][LiCr(ox)_3]$	$[Co(bpy)_3][LiCr(ox)_3]$	$[Ru(bpy)_3][LiCr(ox)_3]$
formula	$C_{36}H_{24}N_6O_{12}NaCrZn$	$C_{36}H_{24}N_6O_{12}NaCrCo$	$C_{36}H_{24}N_6O_{12}LiCrCo$	$C_{36}H_{24}N_6O_{12}LiCrCo$	$C_{36}H_{24}N_6O_{12}LiCrRu$
fw	872.97	866.53	850.48	850.48	892.63
T [K]	293(2)	293(2)	293(2)	10(2)	100(2)
radiation	$Mo_{K\alpha}$	$Mo_{K\alpha}$	$Mo_{K\alpha}$	$Mo_{K\alpha}$	$Mo_{K\alpha}$
crystal system	cubic	cubic	cubic	cubic	cubic
space group	$P2_13$	$P2_13$	$P2_13$	$P2_13$	$P2_13$
a [Å]	15.6365(18)	15.5850(8)	15.3866(8)	15.2230(18)	15.3091(10)
V [Å^3]	3823.1(8)	3785.5(3)	3652.7(3)	3527.8(7)	3588.0(4)
Z	4	4	4	4	4
ρ_{calcd} [g cm^{-3}]	1.517	1.520	1.551	1.601	1.652
ρ_{obs} [g cm^{-3}]	–	1.54	1.55	–	–
μ [cm^{-1}]	9.93	8.08	8.54	8.54	0.798
transmission factor range	0.733–0.784	–	–	0.7607–0.8173	–
F(000)	1772	1760	1728	1728	1796
crystal size [mm]	0.3 × 0.3 × 0.3	0.40 × 0.40 × 0.30	0.33 × 0.33 × 0.23	0.33 × 0.33 × 0.23	0.4 × 0.4 × 0.4
Θ range [°]	2.46–26.6	2.61–25.86	2.29–25.91	2.32–30.04	1.88–26.36
index range, h, k, l	−13/13, 0/14, 1/20	−18/18, −18/19, −19/19	−18/18, −18/17, −18/18	−16/18, −15/15, −21/12	−19/17, −18/19, −11/19
reflcns measured	21275	28228	19023	7322	17822
unique reflcns	2870	2459	2378	3458	2380
R_{int}	0.0587	0.0678	0.0692	0.077	0.037
reflcns used	2870	2459	2378	3458	2355
parameters	181	173	173	173	173
goodness-of-fit on F^2	1.061	0.899	0.846	0.962	1.225
final R_1 and wR_2 on F bas. and F^2, $I > 2\sigma(I)$	0.0357, 0.0906	0.0304, 0.0573	0.0337, 0.0600	0.0683, 0.1003	0.0386, 0.0940
R_1 and wR_2 indices (all data)	0.0528, 0.0996	0.0475, 0.0602	0.0529, 0.0634	0.0888, 0.1088	0.0391, 0.0943
abs. structure param.	−0.004(17)	−0.01(2)	−0.01(3)	0.01(4)	0.05(6)
2nd extinction param.	–	0.0026(3)	0.00041(11)	–	0.0031(9)
max shift/esd	0.001	0.001	0.001	0.004	0.001
min/max peaks [e Å^{-3}]	−0.299, 0.680	−0.196, 0.290	−0.221, 0.475	−1.510, 1.012	−0.589, 1.293

0947-6539/00/0602-0362 $ 17.50+.50/0 *Chem. Eur. J.* **2000**, *6*, No. 2

Table 2. Selected bond lengths and angles for $[Zn(bpy)_3][NaCr(ox)_3]$, $[Co(bpy)_3][NaCr(ox)_3]$ and $[Co(bpy)_3][LiCr(ox)_3]$ at 293 K, and $[Co(bpy)_3][LiCr(ox)_3]$ at 10 K and $[Ru(bpy)_3][LiCr(ox)_3]$ at 100 K.

	$[Zn(bpy)_3][NaCr(ox)_3]$ 293 K	$[Co(bpy)_3][NaCr(ox)_3]$ 293 K	$[Co(bpy)_3][LiCr(ox)_3]$ 293 K	$[Co(bpy)_3][LiCr(ox)_3]$ 10 K	$[Ru(bpy)_3][LiCr(ox)_3]$ 100 K
unit cell parameters					
a [Å]	15.6365(8)	15.5850(8)	15.3866(8)	15.2230(18)	15.3091(10)
V [Å^3]	3823.1	3785.5	3652.7	3527.8(7)	3588.0(8)
bond lengths [Å]					
M^{II}–N1	2.157(2)	2.121(2)	2.096(2)	2.013(4)	2.061(3)
M^{II}–N2	2.154(2)	2.125(2)	2.094(2)	2.015(3)	2.054(4)
Cr–O1	1.973(2)	1.963(2)	1.978(2)	1.988(3)	1.988(4)
Cr–O2	1.966(2)	1.967(2)	1.978(2)	1.981(3)	1.983(4)
M^{I}–O3	2.392(2)	2.340(2)	2.143(6)	2.170(8)	2.163(6)
M^{I}–O4	2.349(2)	2.366(2)	2.321(5)	2.222(7)	2.287(7)
bite angle [°] (Oh: 90°)					
$[M^{II}(bpy)_3]^{2+}$	76.62(8)	77.37(8)	78.10(9)	80.23(15)	79.24
twist angle [°] (Oh: 60°)					
$[M^{II}(bpy)_3]^{2+}$	45.4	47.7	48.9	51.2	49.3

bond lengths are more interesting because in $[Zn(bpy)_3][NaCr(ox)_3]$ and $[Co(bpy)_3][NaCr(ox)_3]$ they are not too different, but they are distinctly smaller and strongly temperature dependent in $[Co(bpy)_3][LiCr(ox)_3]$. In the last compound they decrease from an average of 2.095 Å to 2.014 Å (that is, by 0.081 Å) between 293 and 10 K. This is far too large to be due to thermal contraction alone, and serves as a first indication that $[Co(bpy)_3]^{2+}$ has become a spin-crossover complex in this lattice. The bite and twist angles (defined as the projection of the bite angle onto a plane perpendicular to the trigonal axis) of the $[M^{II}(bpy)_3]^{2+}$ complexes are within the range generally observed for tris-bipyridyl complexes.[8]

Magnetic susceptibility measurements: Figure 2 shows the magnetic susceptibilities in the form of the product χT as a function of temperature for $[Co(bpy)_3][NaCr(ox)_3]$ and $[Co(bpy)_3][LiCr(ox)_3]$. For comparison, the χT values for $[Zn(bpy)_3][NaCr(ox)_3]$ are also included. In this system, χT is almost temperature independent, and takes on values between $1.90\ cm^3 mol^{-1} K$ ($\mu_{eff} = 3.90\ \mu_B$) at 10 K and $2.05\ cm^3 mol^{-1} K$ ($\mu_{eff} = 4.05\ \mu_B$) at 300 K. This is the typical behaviour of a spin-only magnet with $S = ½$, as expected for the $^4A_2$ ground state of the isolated $[Cr(ox)_3]^{3-}$ complexes that are the only spin carriers in this system.

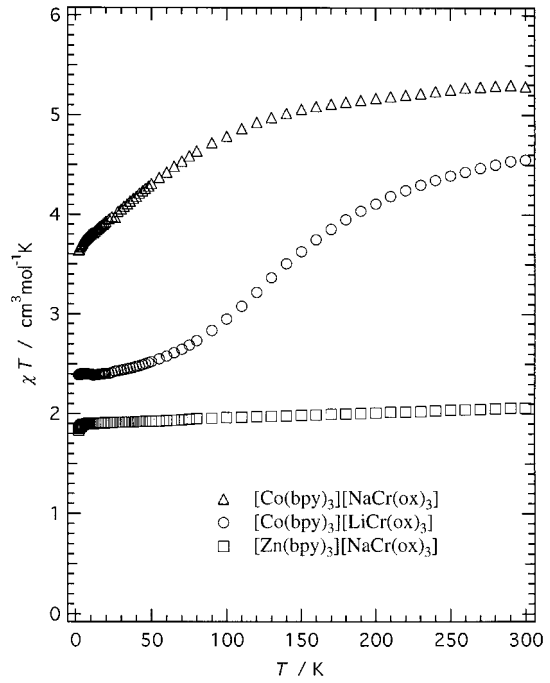

Figure 2. Magnetic susceptibilities of polycrystalline samples of $[Co(bpy)_3][NaCr(ox)_3]$ (△), $[Co(bpy)_3][LiCr(ox)_3]$ (○), and $[Zn(bpy)_3][NaCr(ox)_3]$ (◆) plotted as χT versus temperature.

The χT curves of the two compounds containing $[Co(bpy)_3]^{2+}$ instead of the diamagnetic $[Zn(bpy)_3]^{2+}$ are both strongly temperature dependent, but in very different ways. Subtracting the contribution due to $[Cr(ox)_3]^{3-}$ for $[Co(bpy)_3][NaCr(ox)_3]$ leaves a curve that is typical for $[Co(bpy)_3]^{2+}$ in the $^4T_1$ high-spin state.[9] In the high-spin state, the orbital contribution to the magnetic moment is substantial, resulting in the rather strong temperature dependence of χT. The low-temperature value of χT for the $[Co(bpy)_3]^{2+}$ contribution is $1.8\ cm^3 mol^{-1} K$ ($\mu_{eff} = 3.80\ \mu_B$). This and the high value of the $[Co(bpy)_3]^{2+}$ contribution to χT of $3.23\ cm^3 mol^{-1} K$ ($\mu_{eff} = 5.08\ \mu_B$) at 300 K, in fact, indicate a ligand field very close to octahedral and substantial configuration interaction in the $^4T_1$ states between the ground state ($t_{2g}^5 e_g^2$) and the excited state ($t_{2g}^4 e_g^3$) strong field configurations.[9]

The χT curve of $[Co(bpy)_3][LiCr(ox)_3]$ shows very different behaviour. At 10 K, and after subtraction of the $[Cr(ox)_3]^{3-}$ contribution, the $[Co(bpy)_3]^{2+}$ contribution to χT is a mere $0.5\ cm^3 mol^{-1} K$ ($\mu_{eff} = 2.0\ \mu_B$). This is only slightly above the spin-only value for $S = ½$ of $0.37\ cm^3 mol^{-1} K$ ($\mu_{eff} = 1.73\ \mu_B$), and points to $[Co(bpy)_3]^{2+}$ being in the ^2E low-spin state at 10 K. With increasing temperature, χT increases sigmoidally, and at 300 K it reaches a value of $2.55\ cm^3 mol^{-1} K$ ($\mu_{eff} = 4.52\ \mu_B$). This is still below the value of the typical high-spin compound, but the curve seems to approach that of the high-spin system asymptotically. Thus, the magnetic susceptibility measurements give a clear indication of a thermal spin transition for $[Co(bpy)_3]^{2+}$ in the three-dimensional network $[Co(bpy)_3][LiCr(ox)_3]$.

Optical spectroscopy: Figure 3 (top) shows the single-crystal absorption spectra of $[Zn(bpy)_3][NaCr(ox)_3]$ between 9000

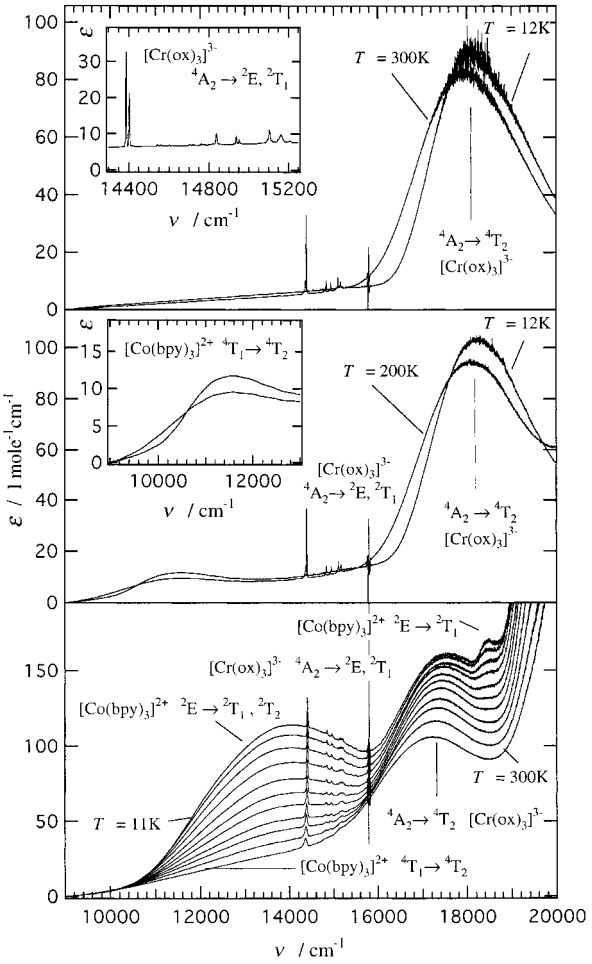

Figure 3. Single crystal absorption spectra of $[Zn(bpy)_3][NaCr(ox)_3]$ (top), $[Co(bpy)_3][NaCr(ox)_3]$ (middle) and $[Co(bpy)_3][LiCr(ox)_3]$ (bottom).

and 20000 cm^{-1} at 12 and 300 K. The only chromophore that absorbs in this spectral region is $[Cr(ox)_3]^{3-}$. On the basis of the work by Schönherr et al.[10] and of the Tanabe–Sugano diagram for a d^3 system,[11] it is straightforward to assign the observed absorption bands. The broad band centred at 18100 cm^{-1} in the spectrum at 12 K corresponds to the spin-allowed $^4A \rightarrow {}^4T_2$ d–d transition, which directly gives the ligand-field strength $10Dq = 18100\ cm^{-1}$. The sharp doublet at 14387 cm^{-1} corresponds to the spin-flip transition $^4A_2 \rightarrow {}^2E$, and the series of sharp and weak bands between 14400 and 15600 cm^{-1} corresponds to the vibrational side bands of the $^4A_2 \rightarrow {}^2E$ transition and the other spin-flip transition $^4A_2 \rightarrow {}^2T_1$.

Figure 3 (middle) shows the single-crystal absorption spectra of $[Co(bpy)_3][NaCr(ox)_3]$ between 9000 and 20000 cm^{-1} at 12 and 200 K. In addition to the bands characteristic of $[Cr(ox)_3]^{3-}$, there is an additional weak band at 11500 cm^{-1}. This has to be due to $[Co(bpy)_3]^{2+}$ since it is totally absent in the compound with $[Zn(bpy)_3]^{2+}$ substituted for $[Co(bpy)_3]^{2+}$. According to the literature,[6, 12] this band is typical for high-spin $[Co(bpy)_3]^{2+}$ both in its energy as well as in its comparatively small oscillator strength of 4×10^{-5}. On the basis of the Tanabe–Sugano diagram[11] for a d^7 system this band can therefore be assigned to the spin-allowed d–d transition $^4T_1 \rightarrow {}^4T_2$. A further point to note for the later discussion is the fact that at 18300 cm^{-1} at 12 K the $^4A_2 \rightarrow {}^4T_2$ transition of $[Cr(ox)_3]^{3-}$ is at a slightly higher energy than in the compound with $[Zn(bpy)_3]^{2+}$ instead of $[Co(bpy)_3]^{2+}$.

Figure 3 (bottom) depicts the single crystal absorption spectra of $[Co(bpy)_3][LiCr(ox)_3]$ between 9000 and 20000 cm^{-1} and at temperatures between 12 and 300 K. Again the bands characteristic of $[Cr(ox)_3]^{3-}$ can easily be assigned. At 12 K the $^4A_2 \rightarrow {}^4T_2$ transition at 17500 cm^{-1} is now at substantially lower energy than in the other two systems, whereas the $^4A_2 \rightarrow {}^2E$ transition at 14408 cm^{-1} is at somewhat higher energy. The most astonishing feature, however, is the comparatively strong, temperature-dependent and slightly asymmetric absorption band centred at 14000 cm^{-1}. This band is most intense at 12 K and decreases in intensity as the temperature increases. At 300 K it is no longer resolvable and just contributes to the sloping background. This band indicates that in $[Co(bpy)_3][LiCr(ox)_3]$ there is a thermal equilibrium between different electronic states peculiar to the $[Co(bpy)_3]^{2+}$. Furthermore it must be due to the low-temperature species and therefore cannot be due to the high-spin state. From the Tanabe–Sugano diagram[11] for a d^7 system, this band can be assigned to the spin-allowed and overlapping d–d transitions of the low-spin species $^2E \rightarrow {}^2T_1{}^a$ and $^2E \rightarrow {}^2T_2$. In addition, there is a weak, temperature-dependent band at 18500 cm^{-1}, which can be tentatively assigned to the second spin-allowed $^2E \rightarrow {}^2T_1{}^b$ transition.

Discussion

The thermal spin transition in $[Co(bpy)_3][LiCr(ox)_3]$: Optical spectroscopy not only supports the assumption of a thermal spin transition based on magnetic susceptibility and crystal structure data, as a probe at a molecular level, but it also proves unambiguously that there is a thermal equilibrium between two electronic states of $[Co(bpy)_3]^{2+}$ in $[Co(bpy)_3][LiCr(ox)_3]$. From the magnetic susceptibility data shown in Figure 2, the fraction of $[Co(bpy)_3]^{2+}$ complexes in the high-spin state, γ_{HS}, as a function of temperature can be calculated from Equation (1), where χ_{obs} is the magnetic susceptibility

$$\gamma_{HS} = \frac{\chi_{obs} - \chi_{LS} - \chi_{Cr^{3+}}}{\chi_{HS} - \chi_{LS} - \chi_{Cr^{3+}}} \quad (1)$$

observed for $[Co(bpy)_3][LiCr(ox)_3]$ as a function of temperature, χ_{HS} is the magnetic susceptibility of the high-spin state, the temperature dependence of which can be taken from the magnetic susceptibility of the high-spin system $[Co(bpy)_3][NaCr(ox)_3]$. By assuming that in $[Co(bpy)_3][LiCr(ox)_3]$ at 10 K all the $[Co(bpy)_3]^{2+}$ complexes are in the low-spin state, the magnetic susceptibility of the low-spin state, χ_{LS}, can be taken from the low-temperature value for this compound, and, finally, for $\chi_{Cr^{3+}}$, the spin-only value observed experimentally for $[Zn(bpy)_3][LiCr(ox)_3]$ can be used. The resulting thermal transition curve is shown in Figure 4. It has the same sigmoidal shape as the χT curve of $[Co(bpy)_3][LiCr(ox)_3]$ itself. At 300 K the high-spin fraction $\gamma_{HS} = 0.75$. The above analysis neglects possible interactions between the $[Co(bpy)_3]^{2+}$ and $[Cr(ox)_3]^{3-}$ entities. However, on the basis

0947-6539/00/0602-0364 $ 17.50+.50/0 Chem. Eur. J. 2000, 6, No. 2

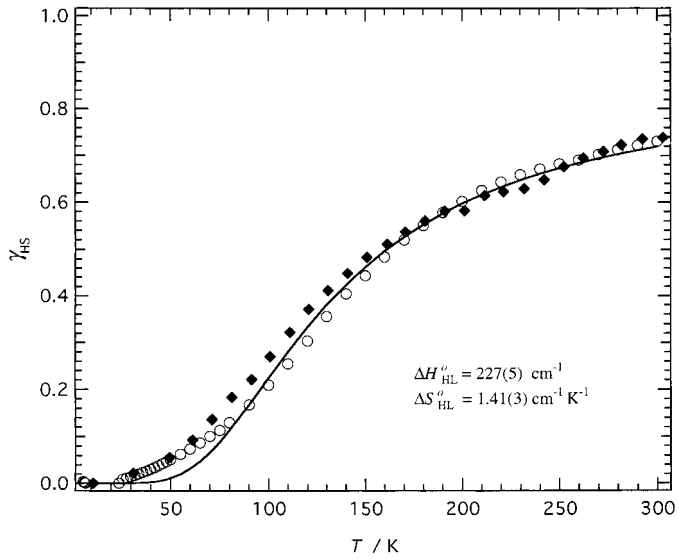

Figure 4. Spin-transition curves of $[Co(bpy)_3][LiCr(ox)_3]$ as determined from magnetic susceptibility (○), optical spectroscopy (◆), and least-squares fitting of the spin equilibrium according to Equation (3) to the experimental points (solid line).

of the observation of energy-transfer properties of the related system containing $[Cr(bpy)_3]^{3+}$ instead of $[Co(bpy)_3]^{2+}$, host–guest interactions by superexchange through π overlap of the respective ligand systems have been estimated to be less than 0.1 cm^{-1}.[13]

A transition curve can also be constructed from the temperature-dependent optical spectra. By assuming that in the noncentrosymmetric complexes the temperature dependence of the oscillator strengths of the spin-allowed d–d transitions is negligible, the high-spin fraction is given by Equation (2), where $I(T)$ is the experimental integrated

$$\gamma_{HS} = \frac{I_{LS} - I(T)}{I_{LS} - I_{HS}} \quad (2)$$

intensity over the spectral range covering the optical transitions of interest, and I_{LS} and I_{HS} are the integrated intensities of the system fully in the low-spin and fully in the high-spin states, respectively. I_{LS} is known from the low-temperature spectrum, but unfortunately I_{HS} is not known. In principle, it could be taken from the $[Co(bpy)_3][NaCr(ox)_3]$ spectrum, but because of i) the inherent problem of sloping base lines in single crystal spectra and ii) the fact that there is a substantial shift in the $^4A \rightarrow {}^4T_2$ transition of $[Cr(ox)_3]^{3-}$ this would not be very accurate. With the quite accurate estimate of γ_{HS} at 300 K of 0.75 from magnetic susceptibility measurements, it is more sensible to treat the factor $(I_{LS} - I_{HS})^{-1}$ as a proportionality constant and to scale γ_{HS} to the above value of 0.75 at 300 K. The resulting transition curve, included in Figure 4, is in good agreement with the one from the magnetic susceptibility measurements.

In $[Co(bpy)_3][LiCr(ox)_3]$ the spin transition is gradual. There are no indications of any strong cooperative effects,[14] nor are there complications from crystallographic phase transitions. However, fitting the thermal transition curve by taking into account just the electronic splittings of the ^2E and the $^4T_1$ states in the trigonal ligand field is not adequate, as the vibrational contribution to the entropy change is expected to be quite large.[14] In this case, the simplest thermodynamic approach to the LS ⇌ HS equilibrium is given in Equation (3).

$$\gamma_{HS} = (1 + e^{\Delta H^0_{HL} - T\Delta S^0_{HL})/k_B T})^{-1} \quad (3)$$

A least-squares fit to the experimental transition curve derived from the magnetic susceptibility measurements yields values for the thermodynamic parameters of 227(5) cm^{-1} (2.72 kJ mol^{-1}) and 1.41(3) cm^{-1} K^{-1} (16.9 J mol^{-1} K^{-1}) for ΔH^0_{HL} and ΔS^0_{HL}, respectively. Whereas the value for ΔH^0_{HL} is in good agreement with the one reported by Tiwary and Vasudevan[4] for $[Co(bpy)_3]^{2+}$ incorporated into zeolite-Y, the value for ΔS^0_{HL} is substantially larger. It is, however, within the range reported by Zarembowitch[15] for several cobalt(II) spin-crossover systems. But as expected, ΔS^0_{HL} is still much smaller than the corresponding typical values in the range from 5 to 10 cm^{-1} K^{-1} for iron(II) spin-crossover systems.[14] This is due to the smaller ratios of both electronic and vibrational degeneracies between the two states for cobalt(II) spin-crossover systems. It should be noted that both ΔH^0_{HL} and ΔS^0_{HL} are not strictly temperature independent because of the splitting of the $^4T_1$ state under the combined effects of spin–orbit coupling and a small trigonal component to the ligand field. The values given here should be regarded as valid at the transition temperature $T_{1/2}$ of 161 K [Eq. (4)], which is defined as the temperature for which $\gamma_{HS} = 0.5$.

$$T_{1/2} = \Delta H^0_{HL} / \Delta S^0_{HL} \quad (4)$$

As mentioned above, there are no direct indications of any cooperative effects driving the spin transition in the present system. Small effects could, however, be responsible for the apparently larger value of ΔS^0_{HL} as compared with the one reported by Tiwary and Vasudevan.[4] On the other hand, the smaller value found by these authors could be an artefact due to an inhomogeneous distribution of the zero-point energy difference between the two electronic states in the zeolite cavity.

Geometric changes: The average Co–N bond length of the high-spin compound $[Co(bpy)_3][NaCr(ox)_3]$ of 2.123 Å is almost identical to the one observed for other compounds containing the $[Co(bpy)_3]^{2+}$ moiety. In $[Co(bpy)_3]Cl_2 \cdot 2H_2O \cdot EtOH$, for instance, it is 2.128 Å.[8] Similarly, the average values of the bite and the twist angle for this compound of 76.5° and 44.9° (calculated from the structure parameters given in ref. [8]), respectively, are only slightly smaller than the values of 77.4° and 47.7° of $[Co(bpy)_3][NaCr(ox)_3]$.

The difference in Co–N bond lengths between the high-spin and the low-spin state, Δr_{HL}, of the spin-crossover system $[Co(bpy)_3][LiCr(ox)_3]$ follows directly from the crystallographic data. At 293 K, the average Co–N bond lengths are 2.095 Å, and at 10 K they are 2.014 Å. The former value corresponds to $\gamma_{HS} = 0$, the latter to $\gamma_{HS} = 0.73$. From this, a value for Δr_{HL} of 0.110 Å can be derived. Thus, the Co–N bond length for the high-spin state is extrapolated to 2.124 Å, which is exactly equal to the one determined for the high-spin

system $[Co(bpy)_3][NaCr(ox)_3]$. The above value of Δr_{HL} is also identical to the 0.11 Å reported as the average value for the difference in Co–N bond lengths for the spin-crossover complex $[Co(terpy)_2]^{2+}$ (terpy = terpyridine).[16] The key difference between this complex and the $[Co(bpy)_3][LiCr(ox)_3]$ system is that for the former the value of $\Delta r_{HL} = 0.11$ Å is made up of the differences in $Co–N_{central}$ of 0.21 Å and the differences in $Co–N_{distal}$ of 0.06 Å, whereas in the latter all six bond lengths change by almost equal amounts. Of course, the bite and twist angles of the $[Co(bpy)_3]^{2+}$ moiety have to respond to the large difference in Co–N bond lengths. Thus already at 293 K both angles are slightly larger than in the corresponding high-spin system $[Co(bpy)_3][NaCr(ox)_3]$, and as the $[Co(bpy)_3]^{2+}$ complex crosses to the low-spin state, there is a further increase towards a less trigonally distorted coordination. In fact, the $[Co(bpy)_3]^{2+}$ complex in this system is by far the most symmetric cobalt(II) spin-crossover complex found to date. Most other cobalt(II) spin-crossover complexes already have a very asymmetric coordination sphere to begin with, such as the class of complexes with Schiff bases derived from 3-formylsalicylic acid with $[CoN_4O_2]$ coordination,[15] and consequently, it is not surprising that the changes in bond length accompanying the spin transition are not all equal. In addition, in such systems the Jahn–Teller effect in the ^2E state helps to drive the static distortion along a normal coordinate that is not totally symmetric.

Ligand-field strengths: The determination of ligand-field strengths from the optical spectra is not straightforward, as none of the observed transitions corresponds directly to $10Dq$. Furthermore, the number of observed transitions is not sufficient for a determination of the Racah parameters B and C and the ligand-field strength $10Dq$ for both the high-spin and the low-spin complexes on the basis of these spectra alone. For the low-spin species in $[Co(bpy)_3][LiCr(ox)_3]$ with two bands assigned, it should, however, be possible to estimate B and $10Dq$ by setting $C \approx 4B$.[17] According to the Tanabe–Sugano diagram for a d^7 system,[11] the energy difference between the two close lying excited states $^2T_1{}^a$ and $^2T_2$, and the next higher excited state $^2T_1{}^b$ ($E(^2T_1{}^b) - E(^2T_1{}^a, {}^2T_2)$ is about $8B$ and is independent of the ligand-field strength in the strong-field limit, because these three states all arise from the same strong-field configuration ($t_{2g}^5 e_g^2$). With the experimental values of the $^2E \rightarrow {}^2T_1{}^a$, $^2T_2$ and $^2E \rightarrow {}^2T_1{}^b$ transitions discussed above (see Optical spectroscopy), $E(^2T_1{}^b) - E(^2T_1{}^a, {}^2T_2) = 4500$ cm^{-1}, from which a value for B of ≈ 565 cm^{-1} can be estimated. In the low-spin complex, B is thus reduced from its free-ion value of 1115 cm^{-1}[17] by an orbital reduction factor of 0.5. With this value of B, the experimental energy difference between the two close lying excited states $^2T_1{}^a$ and $^2T_2$, and the ^2E ground state can be expressed in units of B as $E(^2T_1{}^a, {}^2T_2) - E(^2E)$ to give a value of 14000 cm^{-1} or $25B$. Again, according to the Tanabe–Sugano diagram, this results in a ligand-field strength for the low-spin complex of $10Dq^{LS} \approx 27B$ or 15300 cm^{-1}.

Unfortunately, in the spin-crossover system $[Co(bpy)_3][LiCr(ox)_3]$ no absorption bands of the high-spin state could be resolved, because of the spectral overlap between the comparatively weak spin-allowed, high-spin band and the more intense low-spin band. However, the one absorption band observed for the high-spin system $[Co(bpy)_3][NaCr(ox)_3]$ at 11400 cm^{-1} may also be considered typical for the energy of the $^4T_1 \rightarrow {}^4T_2$ transition of the spin-crossover system. This energy is identical to that of this transition as observed by Palmer and Piper for $[Co(bpy)_3]^{2+}$ in solution.[12] In solution, with no interference from other chromophores, these authors were able to assign a series of bands and to perform a ligand-field analysis, which resulted in values of $B = 790$ cm^{-1}, an orbital reduction factor $\beta = 0.71$, and $10Dq^{HS} = 12700$ cm^{-1}. These values can confidently be transferred to high-spin $[Co(bpy)_3]^{2+}$ in the oxalate networks.

The orbital reduction factor β and thus B vary quite substantially between the two spin states. The value of β for the low-spin state is smaller than the one for the high-spin state. This is not unexpected, as the delocalisation of the d electrons towards ligand orbitals is more pronounced for the low-spin state with its smaller metal–ligand bond lengths.

The values of the ligand-field strengths of the high-spin and the low-spin species, $10Dq^{HS} \approx 12700$ cm^{-1} and $10Dq^{LS} \approx 15300$ cm^{-1}, respectively, can be checked for internal consistency on the basis of the metal–ligand bond length dependence of $10Dq$ on r^{-n}, with $n = 5–6$. With metal–ligand bond lengths of 2.022 and 2.125 Å for the low-spin and the high-spin state, respectively, the expected ratio is ≈ 1.3. This compares reasonably well with the ratio of 1.2 as estimated with the above values of the respective ligand-field strengths. Furthermore, according to the Tanabe–Sugano diagram, the critical ligand-field strength, $10Dq^{crit}$, where the ligand-field stabilisation is equal to the spin-pairing energy π, is at $21.5B$. In a configurational coordinate diagram for a given complex this point corresponds to the crossing point of the diabatic potentials of the high-spin and the low-spin state. For a spin-crossover compound this point has to be approximately halfway between the two potential minima. Thus by taking B at this nuclear configuration to be the mean of the above values for the high-spin and the low-spin state, respectively, a value for $10Dq^{crit}$ of 14400 cm^{-1} can be estimated, which is in between the values of $10Dq^{LS}$ and $10Dq^{HS}$.

In their report, Tiwary and Vasudevan[4] stress the importance of the influence of the zeolite matrix on the trigonal component of the ligand field as the actual force that drives $[Co(bpy)_3]^{2+}$ into becoming a spin-crossover complex. We find no indication to support this assertion. In $[Co(bpy)_3][LiCr(ox)_3]$, the $[Co(bpy)_3]^{2+}$ complexes actually retain their high molecular symmetry. The difference in twist and bite angles between the two states is not very large, but as for the spin-crossover systems of iron(II) and iron(III), it is the change in metal–ligand bond length that is the most striking structural feature. Thus, the reaction coordinate for the spin transition is dominated by the totally symmetric breathing mode of the complex, and the trigonal twist and bite angles just react to satisfy the geometric restraints imposed by the bidentate nature of the bipyridine ligands. It is also true that the trigonal component of the ligand field is quite small in the oxalate networks, as demonstrated by the rather large values of χT of the high-spin compound. The trigonal splitting of the $^4T_1$ state in the $[Co(bpy)_3][NaAl(ox)_3]$ derivative is 350 cm^{-1}, with the $^4A_2$ component below the ^4E component.[18] Both the magni-

0947-6539/00/0602-0366 $ 17.50+.50/0 *Chem. Eur. J.* **2000**, *6*, No. 2

tude and the sign of this splitting are comparable with other tris-bipyridine complexes in the solid state with C_3 site symmetry, such as $[Cr(bpy)_3]^{3+}$,[19] and is in line with the report on $[Co(bpy)_3]^{2+}$ by Palmer and Piper.[12]

Finally, the shifts in the absorption bands of $[Cr(ox)_3]^{3-}$ upon substitution of Na^+ by Li^+ in $[Co(bpy)_3][NaCr(ox)_3]$ need to be discussed briefly. With Li^+, the cavity for the tris-bipyridyl complex is slightly too small for $[Co(bpy)_3]^{2+}$. This is the actual driving force for making this complex a spin-crossover complex in $[Co(bpy)_3][LiCr(ox)_3]$. On the other hand, the tris-bipyridyl complex deforms the cavity to some extent. Thus, the two nonequivalent Li–O bond lengths differ quite substantially, and in $[Co(bpy)_3][LiCr(ox)_3]$ the Cr–O bond lengths are elongated by 0.014 Å with respect to those in $[Co(bpy)_3][NaCr(ox)_3]$. With the r^{-n} dependence of the ligand-field strength, the shift of the $^4A_2 \rightarrow {}^4T_2$ band from 18300 to 17500 cm^{-1} corresponds exactly to the decrease in $10Dq$ due to this elongation. At the same time, there is a slight increase in the orbital reduction factor associated with the larger metal–ligand bond lengths. As a result, a small shift of 21 cm^{-1} to higher energy is observed for the ligand-field strength independent spin-flip $^4A_2 \rightarrow {}^2E$ transition.

Conclusion

We have demonstrated the phenomenon of a thermal spin transition for the $[Co(bpy)_3]^{2+}$ complex in $[Co(bpy)_3][LiCr(ox)_3]$. A coherent and internally consistent picture taking into account structural data, magnetic susceptibility measurements and optical absorption spectra has been developed, which shows how host–guest interactions influence the electronic energies of each other.

As mentioned above, in principle the ^2E state is subject to the Jahn–Teller effect. Whereas in less symmetric systems this results in strong tetragonal distortions, the $[Co(bpy)_3]^{2+}$ complex in $[Co(bpy)_3][LiCr(ox)_3]$ retains its C_3 site symmetry even in the low-spin state. This does not necessarily mean that the Jahn–Teller effect is not active. The rather tight fit of the $[Co(bpy)_3]^{2+}$ complexes in the oxalate network just prevents a static, and thus cooperative, distortion. Unfortunately, with the $[Cr(ox)_3]^{3-}$ present in high concentrations, spin–spin relaxation prevents the recording of meaningful EPR spectra in $[Co(bpy)_3][LiCr(ox)_3]$ in order to check for a dynamic Jahn–Teller effect.

In an astonishing number of cobalt(II) spin-crossover compounds cooperative effects lead to quite large thermal hysteresis behaviour. This is in all probability due to the anisotropic change in the actual shape of the complexes themselves, and leads to strong nearest neighbour interactions[20] and cooperative Jahn–Teller distortions.[15] In contrast, in the high symmetry compound $[Co(bpy)_3][LiCr(ox)_3]$, cooperative effects are restricted to the long-range contribution in the form of an image pressure.[21] Such long-range interactions are directly related to the difference in volumes between the high-spin and the low-spin states. As both the difference in bond lengths as well as the difference in volumes are smaller in cobalt(II) when compared with iron(II) spin-crossover complexes, the long-range contribution for the former is expected to be small, and indeed in $[Co(bpy)_3][LiCr(ox)_3]$ the spin transition is gradual without any indications of large cooperative effects. It would, nevertheless, be interesting to follow up on this aspect by studying a metal dilution series of the form $[M_{1-x}Co_x(bpy)_3][LiCr(ox)_3]$, where M is an innocent metal ion such as zinc(II) or iron(II). Since the influence of substituting Na^+ by Li^+ has been ascribed to an increasing internal pressure, it would also be interesting to study the effects of an external pressure on both $[Co(bpy)_3][LiCr(ox)_3]$ and $[Co(bpy)_3][NaCr(ox)_3]$. These cubic compounds are particularly suited to pressure studies under hydrostatic pressure, and a comparatively small external pressure might be sufficient to push the high-spin system $[Co(bpy)_3][NaCr(ox)_3]$ into becoming a spin-crossover system.

Experimental Section

Sample preparation: Samples in the form of polycrystalline powders were prepared by adapting the procedures previously described. Single crystals in the form of perfect tetrahedra with edges of up to 0.4 mm were grown by slow diffusion in a silicate gel.[22]

X-ray diffraction studies: The relevant structure determination parameters are given in Table 1. Single-crystal data for $[Zn(bpy)_3][NaCr(ox)_3]$ at 293 K and for $[Ru(bpy)_3][LiCr(ox)_3]$ at 100 K were collected on a Siemens Smart-CCD diffractometer and for $[Co(bpy)_3][NaCr(ox)_3]$ and $[Co(bpy)_3][LiCr(ox)_3]$ at 293 K on a Stoe Image Plate Diffraction System with graphite-monochromated $Mo_{K\alpha}$ radiation ($\lambda = 0.71073$ Å). The 10 K data for $[Co(bpy)_3][LiCr(ox)_3]$ were collected on an Fddd diffractometer,[23] which consists of an APD 202 Displex cryogenic refrigerator on a Huber 512 goniometer with an offset χ-circle, a Bruker Mo rotating anode generator ($\lambda = 0.71073$ Å) and a fast scintillation detector. A dark red crystal was attached to a sharpened graphite rod (0.3 mm) by means of a low-temperature epoxy glue and was mounted on the Displex. The crystal was cooled to and maintained at 10 K. Data were collected by using ω-2θ scans. Three standard reflections were measured every 100 reflections and showed ca. 6% variation over the entire data collection.

The structures were solved by direct methods in the program SHELXS97[24] and refined by full-matrix least-squares on F^2 with the program SHELXL97.[25] The hydrogen atoms were included in calculated positions and treated as riding atoms by means of SHELXL97 default parameters. The final refinements—for the measurements at 293 as well as at 100 K of the four compounds—converged to $R_1 < 0.036$ and $wR_2 < 0.091$ for the observed data [$I > 2\sigma(I)$]. The refinement of the structure of $[Co(bpy)_3][LiCr(ox)_3]$ at 10 K converged at $R_1 = 0.068$ and $wR_2 = 0.1088$ for the observed data [$I > 2\sigma(I)$]. Numerical absorption corrections were applied in the case of $[Zn(bpy)_3][NaCr(ox)_3]$, and for the structure of $[Co(bpy)_3][LiCr(ox)_3]$ at 10 K.

Crystallographic data (excluding structure factors) for the structures reported in this paper have been deposited with the Cambridge Crystallographic Data Centre as supplementary publication nos. CCDC 118927–118931. Copies of the data can be obtained free of charge on application to CCDC, 12 Union Road, Cambridge CB1 1EZ, UK (fax: (+44) 1223-226-033; e-mail: deposit@ccdcd.cam.ac.uk).

Magnetic susceptibility: Magnetic susceptibility measurements between 2 and 300 K were performed on a SQUID MPMS-XL (Quantum Design) with powder samples (between 10 and 40 mg). Diamagnetic corrections were applied by using tabulated Pascal constants.[26]

Optical spectroscopy: Single-crystal absorption spectra between 9000 and 22000 cm^{-1} were recorded on a Fourier transform spectrometer equipped with the appropriate light sources, beam splitters and detectors (Bruker IFS66). To this end, one cap of a perfectly tetrahedral crystal with an edge length of $\approx$0.3 mm was polished off, in order to provide the two parallel faces required for absorption measurements. Temperatures between 11 and 300 K were achieved with a closed-cycle cryosystem with the sample sitting in He exchange gas (Oxford Instruments CCC 1204).

Acknowledgements

We thank the participants of the practical course in X-ray crystallography at the University of Bern[27] for the determination of the crystal structure of the zinc(II) compound. This work was financially supported by the "Schweizerischer Nationalfonds", the "Fondation Ernst et Lucie Schmidheiny", and the "Bundesamt für Forschung und Wissenschaft" within a European Union TMR network.

[1] S. Decurtins, H. W. Schmalle, R. Pellaux, P. Schneuwly, A. Hauser, *Inorg. Chem.* **1996**, *35*, 1451.
[2] a) R. Pellaux, H. W. Schmalle, R. Huber, P. Fischer, T. Hauss, B. Ouladdiaf, S. Decurtins, *Inorg. Chem.* **1997**, 26, 2301; b) S. Decurtins, H. W. Schmalle, P. Schneuwly, R. Pellaux, J. Ensling, *Mol. Cryst. Liq. Cryst.* **1995**, *273*, 167.
[3] a) A. Hauser, M. E. von Arx, R. Pellaux, S. Decurtins, *Mol. Cryst. Liq. Cryst.* **1996**, *286*, 225; b) M. E. von Arx, A. Hauser, H. Riesen, R. Pellaux, S. Decurtins, *Phys. Rev. B* **1996**, *54*, 15800.
[4] a) S. K. Tiwary, S. Vasudevan, *Chem. Phys. Lett.* **1997**, *277*, 84; b) S. K. Tiwary, S. Vasudevan, *Inorg. Chem.* **1998**, *37*, 5239.
[5] K. Mizuno, J. H. Lunsford, *Inorg. Chem.* **1983**, *22*, 3484.
[6] A. B. P. Lever, *Inorganic electronic spectroscopy*, 2nd ed., Elsevier, Amsterdam, **1984**, p. 421ff.
[7] M. E. von Arx, S. C. Capelli, unpublished results.
[8] D. J. Szalda, C. Creutz, D. Mahajan, N. Sutin, *Inorg. Chem.* **1983**, *22*, 2372.
[9] B. N. Figgis, *Progr. Inorg. Chem.* **1964**, *6*, 37.
[10] T. Schönherr, J. Spanier, H.-H. Schmidtke, *J. Phys. Chem.* **1989**, *93*, 5959.
[11] S. Sugano, Y. Tanabe, H. Kamimura, *Multiplets of transition-metal ions in crystals*, Academic Press, London, **1970**, p. 147ff.
[12] R. A. Palmer, T. S. Piper, *Inorg. Chem.* **1966**, *5*, 864.
[13] V. S. Langford, M. E. von Arx, A. Hauser, *J. Phys. Chem. A*. **1999**, *103*, 7161.
[14] a) P. Gütlich, *Struct. Bonding (Berlin)* **1981**, *44*, 83; b) E. König, *Progr. Inorg. Chem.* **1987**; c) E. König, *Struct. Bonding (Berlin)* **1991**, *76*, 51; d) J. K. Beattie, *Adv. Inorg. Chem.* **1988**, *32*, 1.
[15] a) J. Zarembowitch, *New J. Chem*. **1992**, *16*, 255; b) P. Thuéry, J. Zarembowitch, A. Michalowicz, O. Kahn, *Inorg. Chem*. **1987**, *26*, 851.
[16] B. N. Figgis, E. S. Kucharski, A. H. White, *Aust. J. Chem*. **1983**, *36*, 1537.
[17] J. S. Griffith, *The Theory of Transition Metal Ions*, Cambridge University Press, **1971**.
[18] H. Bill, R. Sieber, A. Hauser, unpublished results.
[19] A. Hauser, M. Mäder, W. T. Robinson, R. Murugesan, J. Ferguson, *Inorg. Chem.* **1987**, *26*, 1331.
[20] a) N. Willenbacher, H. Spiering, *J. Phys. C: Solid State Phys.* **1988**, *21*, 1423; b) H. Spiering, N. Willenbacher, *J. Phys. Condens. Matter* **1989**, *1*, 10089.
[21] H. Spiering, E. Meissner, H. Köppen, E. W. Müller, P. Gütlich, *Chem. Phys.* **1982**, *68*, 65.
[22] S. Decurtins, H. W. Schmalle, P. Schneuwly, J. Ensling, P. Gütlich, *J. Am. Chem. Soc.* **1994**, *116*, 9521.
[23] R. C. B. Copley, A. E. Goeta, C. W. Lehmann, J. C. Cole, D. M. Yufit, J. A. K. Howard, *J. Appl. Crystallogr.* **1997**, *30*, 413.
[24] G. M. Sheldrick, SHELXS97, Program for the determination of crystal structures, University of Göttingen, Germany, **1997**.
[25] G. M. Sheldrick, SHELXL97, Program for the refinement of crystal structures, University of Göttingen, Germany **1997**.
[26] A. Earnshaw, *Introduction to Magnetochemistry*, Academic Press, London, **1963**.
[27] S. C. Capelli, J. Hauser, H.-B. Bürgi, practical course in X-ray crystallography, University of Bern, **1998**.

Received: April 26, 1999 [F1744]

  0947-6539/00/0602-0368 $ 17.50+.50/0